



Frequency-Domain Antiferromagnetic Resonance Spectroscopy of NiO

Ohmichi, Eiji
Shoji, Yuto
Takahashi, Hideyuki
Ohta, Hitoshi

(Citation)

Journal of the Physical Society of Japan, 91(9):095001

(Issue Date)

2022-09-15

(Resource Type)

journal article

(Version)

Accepted Manuscript

(Rights)

©2022 The Physical Society of Japan

(URL)

<https://hdl.handle.net/20.500.14094/0100476846>



Frequency-Domain Antiferromagnetic Resonance Spectroscopy of NiO

Eiji Ohmichi¹*, Yuto Shoji¹, Hideyuki Takahashi² and Hitoshi Ohta^{1,2}

¹*Graduate School of Science, Kobe University, 1-1 Rokkodai-cho, Nada, Kobe 657-8501, Japan*

²*Molecular Photoscience Research Center, Kobe University, 1-1 Rokkodai-cho, Nada, Kobe 657-8501, Japan*

The frequency-domain antiferromagnetic resonance (AFMR) of nickel oxide (NiO), known as a typical easy-plane-type antiferromagnet, was investigated using a continuous-wave terahertz spectroscopy technique. The field dependence of the AFMR mode was found to exhibit distinct behavior, depending on the field orientation.

Nickel oxide (NiO) is a typical transition-metal-oxide antiferromagnet with a Néel temperature of $T_N = 525$ K. Recently, NiO has gained considerable attention due to its capacity for ultrafast manipulation of electron spins by ultrashort-pulse lasers.¹⁾ The single crystal has a face-centered rocksalt-type cubic structure in the paramagnetic phase. Electron spins of the Ni^{2+} ion in the antiferromagnetic phase are ferromagnetically aligned within the (111) planes, which are stacked along the $\langle 111 \rangle$ axis alternately to form an easy-plane-type antiferromagnetic order. On the basis of neutron scattering and X-ray experiments on single crystals, it is now conceived that the easy axis within the (111) plane is along the $\langle 11\bar{2} \rangle$ direction.^{2,3)}

Despite its simple crystal structure, the antiferromagnetic resonance (AFMR) spectra of NiO have yet to be fully understood. In NiO, an AFMR mode was clearly observed around 1 THz⁴⁻⁶⁾ (hereafter called the higher AFMR mode), and this higher mode was often analyzed within the framework of the two-sublattice model.⁷⁾ In this model, the spin Hamiltonian is composed of the exchange and anisotropy terms to reproduce the observed AFMR mode. Anisotropy of the former exchange term plays a minor role in this model because the rhombohedral distortion accompanied by the AF order is small. The magnetization measurement suggests a spin-flop transition at 5 K, thus favoring the two-sublattice model.⁸⁾ On the other hand, a total of five AFMR modes, incompatible with the two-sublattice model, were reported as a result of optical measurements.⁹⁻¹¹⁾ Thus, an alternative, eight-sublattice model was proposed, in which the dipolar interactions play a vital role.⁹⁾ It should be also noted that

*ohmichi@harbor.kobe-u.ac.jp

single-crystalline NiO is usually composed of 12 magnetic domains called T -domains and S -domains: T -domains (T_1 - T_4) are related to the four (111)-associated planes, while S -domains (S_1 - S_3) are related to the three $\langle 11\bar{2} \rangle$ -associated directions within each T -domain.¹²⁾

From the viewpoint of antiferromagnetic spintronics,^{13,14)} NiO has been considered a promising candidate because of its high T_N and high AFMR frequency. Therefore, more detailed insight into the magnetic structure of NiO is strongly desired for such forthcoming applications. To this end, it is important to measure the field dependence of the AFMR modes, from which microscopic parameters can be deduced. However, a comprehensive investigation of the frequency-field diagram of NiO has not been performed. This is because AFMR modes showing little field dependence, as is the case for NiO,⁴⁾ are difficult to observe in the conventional setup in which the magnetic field is swept under the irradiation of monochromatic electromagnetic waves.

To overcome this problem, a novel frequency-domain spectroscopy technique, which was recently developed by our group,¹⁵⁾ was applied to a single crystalline NiO in this study. In this Short Note, we report for the first time the magnetic-field diagram of the higher AFMR mode of NiO for three different field orientations in magnetic fields up to 10 T.

In our setup, continuous THz waves were generated by irradiation of THz beats composed of two slightly detuned laser lights onto a photoconductive antenna. This technique allows seamless frequency tuning in the range of 0.05-1.1 THz, thus giving higher resolution than that obtained by THz time-domain spectroscopy. In AFMR spectroscopy, a sample is placed at the magnetic field center, and the transmitted amplitudes of THz waves through the sample are monitored as a function of frequency in a fixed magnetic field.

A (100)-oriented NiO single crystal was used in this study. The sample size was $10 \times 10 \times 5$ mm³. All measurements were carried out at room temperature. The magnetic field dependence of the AFMR mode was measured for three different field orientations along the specific axis: $B//\langle 100 \rangle$, $\langle 110 \rangle$, and $\langle 111 \rangle$, where B is the applied magnetic flux density. The crystal axes were carefully aligned using a specially designed sample holder, and the alignment errors were estimated to be less than a few degrees.

Figure 1 shows typical results of frequency-domain AFMR spectroscopy of NiO for the respective field orientations. Since periodic oscillations of the photocurrent amplitude due to optical interference were visible for $B//\langle 111 \rangle$ and $\langle 110 \rangle$, they were filtered out using the fast Fourier transform algorithm. A small dip observed at 1.1 THz was attributed to water vapor absorption.

At zero magnetic field, a sharp dip was observed around 1 THz, in good agreement with

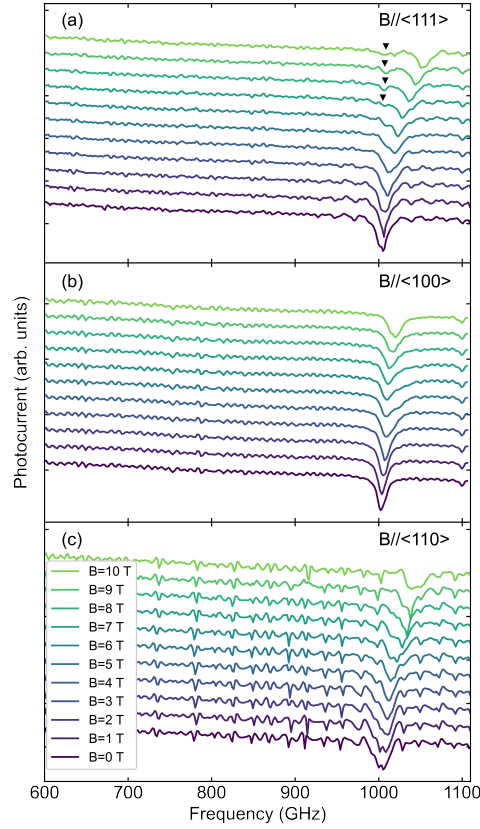


Fig. 1. Room-temperature frequency-domain AFMR spectroscopy of NiO for (a) $B//\langle 111 \rangle$, (b) $B//\langle 100 \rangle$, and (c) $B//\langle 110 \rangle$ in various magnetic fields. The data are vertically shifted for clarity. (Color online)

the previous reports.⁴⁻⁶⁾ As the magnetic field increased, the AFMR mode for $B//\langle 111 \rangle$ started to split into two branches, as shown in Fig. 1(a). One was almost field-independent, while the other showed a quadratic shift to the high-frequency side. In contrast, no splitting was observed for $B//\langle 100 \rangle$ and $\langle 110 \rangle$, as shown in Figs. 1(b) and (c). In the former case, the AFMR mode showed a slight increase, while a quadratic shift was observed in the latter case. It should be noted that such a slightly field-dependent mode could be observed only when the frequency-domain AFMR technique was adopted. We carefully searched for the lower AFMR modes, but could not find corresponding modes below 0.6 THz. In Fig. 2, we summarize the frequency-field diagram of NiO along the respective field orientations.

According to time-resolved Faraday measurements by Wang *et al.*,¹⁶⁾ a similar splitting of the higher AFMR mode was obtained for $B//\langle 111 \rangle$, though the spectral resolution was worse than our results. The magnetic field dependence of the lower AFMR modes was reported from Brillouin scattering measurements.¹⁷⁾ These results were analyzed on the basis of the eight-sublattice model, in which exchange, dipolar, and cubic anisotropy terms were taken into account. The significance of the dipolar interaction in NiO has been claimed for decades,¹⁸⁻²⁰⁾ although it has not been properly considered in the two-sublattice model. In the

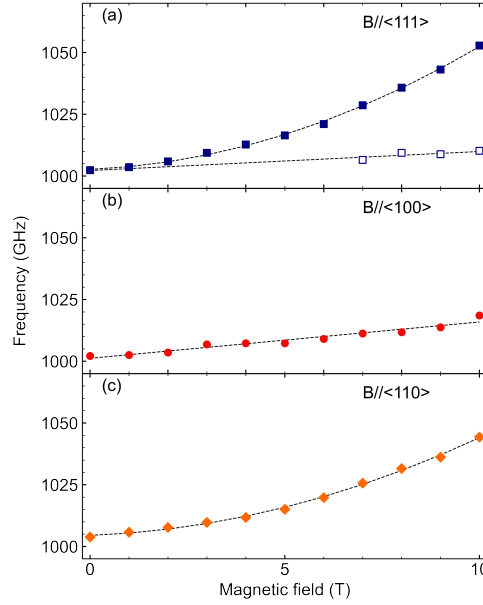


Fig. 2. Frequency-field diagram of NiO for (a) $B//\langle 111 \rangle$, (b) $B//\langle 100 \rangle$, and (c) $B//\langle 110 \rangle$, obtained from Fig. 1. Dotted lines are guides for eyes. (Color online)

eight-sublattice model, dipolar interaction plays an important role in the magnetic anisotropy, so that distinct magnetic field dependences of the AFMR mode, different from those in the two-sublattice model, are expected.

In the following, we compare our results with predictions from the eight-sublattice model. The important point is that in the eight-sublattice model, some of the magnetic domains¹²⁾ become unstable upon application of a magnetic field and will be reoriented above a certain magnetic field, depending on the field direction. In addition, there are three degenerate doublets in the eight AFMR modes. The degeneracy of these doublets will be lifted for certain field orientations.

The most interesting case is when the magnetic field is applied along the $\langle 100 \rangle$ axis. A simulation¹⁷⁾ showed that all of the domain structure for $B//\langle 100 \rangle$ finally becomes unstable and is forced to reorient to the $\langle 01\bar{1} \rangle$ directions above 6.8 T. If this is the case, the higher AFMR mode would show some anomalies around the corresponding field. Besides, considering that the higher AFMR mode is composed of one singlet and one doublet in the eight-sublattice model,⁹⁾ it would be likely that the higher AFMR mode shows some indications of field-induced splitting or broadening. However, neither was observed in our results, as shown in Fig. 2(b), where the AFMR mode shows a small and monotonous shift. Therefore, it seems that the eight-sublattice model alone does not entirely explain our results shown above.

On the other hand, from an analysis based on the two-sublattice model, and taking all

of the magnetic domains into account, a splitting of the higher AFMR mode is expected for both $B//\langle 111 \rangle$ and $\langle 110 \rangle$, which is inconsistent with the observed results. Thus, further investigation is necessary to clarify the magnetic structure of NiO.

Acknowledgment

We thank T. Kohmoto for supplying a single crystal of NiO, and E. Matsuoka for taking Laue photographs. This study was partly supported by a Grant-in-Aid for Scientific Research (B) (No. 21H01040), the Murata Science Foundation, and the Amada Foundation.

References

- 1) P. Němec, M. Fiebig, T. Kampfrath, and A. V. Kimel, *Nature Phys.* **14**, 229 (2018).
- 2) M. T. Hutchings and E. Samuelsen, *Phys. Rev. B* **6**, 3447 (1972).
- 3) T. Yamada, S. Saito, and Y. Shimomura, *J. Phys. Soc. Jpn.* **21**, 672 (1966).
- 4) A. J. Sievers III and M. Tinkham, *Phys. Rev.* **129**, 1566 (1963).
- 5) H. Kondoh, *J. Phys. Soc. Jpn.* **15**, 1970 (1960).
- 6) T. Moriyama, K. Hayashi, K. Yamada, M. Shima, Y. Ohya, and T. Ono, *Phys. Rev. Mat.* **3**, 051402(R) (2019).
- 7) S. M. Rezende, A. Azevedo, and R. L. Rodríguez-Suárez, *J. Appl. Phys.* **126**, 151101 (2019).
- 8) F. L. A. Machado, P. R. T. Ribeiro, J. Holanda, R. L. Rodríguez-Suárez, A. Azevedo, and S. M. Rezende, *Phys. Rev. B* **95**, 104418 (2017).
- 9) J. Milano, L. B. Steren, and M. Grimsditch, *Phys. Rev. Lett.* **93**, 077601 (2004).
- 10) M. Takahara, H. Jinn, S. Wakabayashi, T. Moriyasu, and T. Kohmoto, *Phys. Rev. B* **86**, 094301 (2012).
- 11) T. Satoh, S.-J. Cho, R. Iida, T. Shimura, K. Kuroda, H. Ueda, Y. Ueda, B. A. Ivanov, F. Nori, and M. Fiebig, *Phys. Rev. Lett.* **105**, 077402 (2010).
- 12) I. Sängér, V. V. Pavlov, M. Bayer, and M. Fiebig, *Phys. Rev. B* **74**, 144401 (2006).
- 13) T. Jungwirth, X. Marti, P. Wadley, and J. Wunderlich, *Nature Nanotech.* **11**, 231 (2016).
- 14) V. Baltz, A. Manchon, M. Tsoi, T. Moriyama, T. Ono, and Y. Tserkovnyak, *Rev. Mod. Phys.* **90**, 015005 (2018).
- 15) E. Ohmichi, Y. Shoji, H. Takahashi, and H. Ohta, *Appl. Phys. Lett.* **119**, 162404 (2021).
- 16) Zhe Wang, S. Kovalev, N. Awari, Min Chen, S. Germanskiy, B. Green, J.-C. Deinert, T. Kampfrath, J. Milano, and M. Gensch, *Appl. Phys. Lett.* **112**, 252404 (2018).
- 17) J. Milano and M. Grimsditch, *Phys. Rev. B* **81**, 094415 (2010).
- 18) J. Kaplan, *J. Chem. Phys.* **22**, 1709 (1954).
- 19) F. Keffer and O'Sullivan, *Phys. Rev.* **108**, 637 (1957).
- 20) T. Yamada, *J. Phys. Soc. Jpn.* **21**, 650 (1966).